

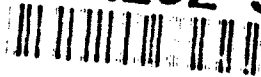
20000920327

REPORT DOCUMENTATION PAGE

Form Approved

OMB No 0704-0183

AD-A262 377



Information is estimated to average 1 hour per response, including the time for reviewing instructions, searching existing data sources, gathering and reviewing the collection of information, Send comments regarding this burden estimate or any other aspect of this collection of information, including suggestions for reducing this burden, to Washington Headquarters Services, Directorate for Information Operations and Reports, 1215 Jefferson Davis Highway, Suite 1204, Arlington, VA 22202-4302, and to the Office of Management and Budget, Paperwork Reduction Project (0704-0183), Washington, DC 20503.

2. REPORT DATE 11 Dec 92 3. REPORT TYPE AND DATES COVERED Quarterly 1 July 92 - 30 Sept. 92

4. TITLE AND SUBTITLE

Optoelectronic Materials Center, A Collaborative Program Including University of New Mexico, Stanford University and California Institute of Technology

5. FUNDING NUMBERS

MDA972-90-C-0046

6. AUTHOR(S)

S.R.J. Brueck, Editor

DTIC

MAR 17 1993

7. PERFORMING ORGANIZATION NAME(S) AND ADDRESS(ES)

University of New Mexico
Center for High Technology Materials
EECE Building, Room 125
Albuquerque, NM 87131-8061

8. PERFORMING ORGANIZATION REPORT NUMBER

9. SPONSORING/MONITORING AGENCY NAME(S) AND ADDRESS(ES)

Defense Advanced Research Projects Agency (DARPA)
ARPA Order No. 7526 Issued by DARPA/CNMO
under Contract #MDA972-90-C-0046

10. SPONSORING/MONITORING AGENCY REPORT NUMBER

11. SUPPLEMENTARY NOTES

12a. DISTRIBUTION/AVAILABILITY STATEMENT

Approved for Public Release Distribution Unlimited

12b. DISTRIBUTION CODE

13. ABSTRACT (Maximum 200 words)

The Optoelectronic Materials Center is a collaborative program involving the University of New Mexico, Stanford University, and the California Institute of Technology. Sandia National Laboratories and MIT Lincoln Laboratory are also involved in this program under separate contract vehicles. This program emphasizes three main areas: 1. diode-based visible sources, 2. two-dimensional optical interconnects, and 3. high-speed optoelectronics.

Progress on individual tasks is discussed briefly in this report. Several tasks affect more than one of the above areas. For simplicity, the tasks are arranged in institution in an order roughly determined by the above areas.

14. SUBJECT TERMS

diode-based visible sources, two dimensional optical interconnects, high-speed optoelectronics

9 plus cover

15. PRICE CODE

17. SECURITY CLASSIFICATION OF REPORT

18. SECURITY CLASSIFICATION OF THIS PAGE

19. SECURITY CLASSIFICATION OF ABSTRACT

20. LIMITATION OF ABSTRACT

Reproduced From
Best Available Copy

98 3 16 084

93-05463



Sponsored by
DEFENSE ADVANCED RESEARCH PROJECTS AGENCY

OPTOELECTRONICS MATERIAL CENTER

A Collaborative Program Including

**Center for High Technology Materials
of the University of New Mexico**

Stanford University

California Institute of Technology

ARPA Order No. 7526
Issued by DARPA/CMO under contract #MDA972-90-C-0046

CLEARED
FOR OPEN PUBLICATION

FEB 17 1993 3

**DIRECTORATE FOR FREEDOM OF INFORMATION
AND SECURITY REVIEW (OASD-PA)
DEPARTMENT OF DEFENSE**

The views and conclusions contained in this document are those of the authors and should not be interpreted as representing the official policies, either express or implied, of the Defense Advanced Research Projects Agency or the U.S. Government.

DARPA OPTOELECTRONICS CENTER

QUARTERLY REPORT

July 1, 1992 through September 30, 1992

UNIVERSITY OF NEW MEXICO

CENTER FOR HIGH TECHNOLOGY MATERIALS

Vertical Cavity Surface-Emitting Lasers

Advances were made in further improving the electrical characteristics of vertical-cavity surface-emitting lasers (VCSELs) during this period. We have previously shown that by grading all the heterointerfaces in the VCSEL epilayer structure, low series resistance and low threshold voltages could be achieved. However, the latter remained significantly above 2V and were dependent on the active area. Theoretical modeling of the electrical resistance carried out during this period suggested that further reduction in the total series resistance and in the threshold voltage are possible. The spreading resistance is a function of the VCSEL device design as well as the proton implantation conditions, which are being varied. The contact resistance, on the other hand, is strictly a function of the metal, semiconductor interface. By tailoring the contact semiconductor layer and refining the interface conditions, we have shown that the threshold voltage can be uniformly reduced below 2V, independent of the VCSEL active area diameter. The fact that this can be achieved without resorting to more complicated structures requiring dielectric multilayer reflectors results in higher-performance devices and a more robust, manufacturable process.

The variations in VCSEL characteristics have also been studied by evaluating both the extent and the nature of the mode mismatch with respect to the gain peak across an epitaxially grown VCSEL wafer. Insight into the mismatch problem was gained from studying the temperature dependence of the lasing threshold current density for VCSELs with different active areas and different initial mode mismatch. Even for devices without any significant initial detuning, cw electrical operation produces thermal self-heating that shifts the gain peak to a wavelength that is substantially longer than the cavity mode. The experimental data showed that these lasers can be thermally-tuned, *i.e.*, restored to a tuned condition by reducing the ambient temperature. (Cheng)

Based on previous experimental results on theoretical analysis and optimization of structure parameters, a novel optically pumped vertical cavity surface emitting laser (VCSEL) has been designed. The gain section is composed of InGaAs/GaAs multiple-quantum-well strained layers. It is designed for very low threshold pumping power density and wide

pumping linewidth, which are critical for optical pumping with edge-emitting high power diode lasers. (McInerney)

Picosecond Pulse Generated from Semiconductor Laser by Regenerative Gain Switching

Generation of stable trains of picosecond pulses from CW semiconductor lasers has been achieved using a novel regenerative gain-switching and mode-locking technique. Pulse durations of less than 35 ps and tuning of the pulse repetition rate from ~200 - 500 MHz, have been demonstrated from the regenerative gain-switched semiconductor laser diode. A pulse width as short as 10 ps has been achieved from regenerative mode-locking laser diode with a repetition rate of 500 MHz. A peak power of more than 50 mW has been achieved in both cases. (McInerney, Jain)

Visualization of Complex 3D Integrated Circuits

Our objective is to freeze in time (on a ps or fs time scale) a two dimensional distribution of fields on a circuit (single shot). Our approach uses field induced second harmonic generation in PLZT thin films.

The main technical problems are: 1) how to apply such a film on the circuit and 2) what is the temporal resolution (how fast does the material respond to the applied electric field?)

Some results were reported in the previous periods with thin films sputtered on sapphire and then pressed onto the circuit surface. As a result of the difficulty of maintaining a uniform contact with an imperfect planicity of the semiconductor, the results were not reproducible. In this period, we succeeded in depositing good films using a simple sol-gel technique.

To determine the temporal resolution, ps pulses were applied to a photoconductive switch of a coplanar stripline. The field was probed 100 μm down the stripline with a delayed probe through the PLZT film. The PLZT response to the applied electric field was found to be instantaneous on the time scale of the pulse. We conclude thus that the change in symmetry leading to a field induced second harmonic occurs in less than 70 ps. This response time will be probed on a shorter time scale in the next quarter. (Diels)

Surface Normal Second Harmonic Generation

We have continued our studies of the blue surface normal second harmonic generation. By studying the wavelength dependence of the optimized resonant structure reported last period, we were able to verify the interference effect predicted by the modeling. The wavelength dependence of the second harmonic output power showed two peaks as predicted by our theory. The maximum output was 700 pW at 485 nm for 110 μW of fundamental in the cavity. This was considerably more than we had previously observed in the green from a single layer waveguide (20W) although our modeling predicts a factor of ten better performance from a multilayer green waveguide over a multilayer blue.

We have also begun measurements of the magnitude and dispersion of $\chi^{(2)}$ in $\text{Al}_x\text{Ga}_{1-x}\text{As}$ as a function of Al composition. We are using surface reflective second harmonic generation normalized to LiNbO_3 or to GaAs. Preliminary results show that $\text{Al}_{0.5}\text{Ga}_{0.5}\text{As}$ has a 50% higher $\chi^{(2)}$ than GaAs in the 700-800 nm fundamental wavelength range. We attribute this to a joint optical density of states resonance (E1) occurring at the second harmonic in $\text{Al}_{0.5}\text{Ga}_{0.5}\text{As}$. $\text{Al}_{0.9}\text{Ga}_{0.1}\text{As}$ has a lower $\chi^{(2)}$ than GaAs in this wavelength range, as expected from fundamental gap considerations. (Malloy)

Thermal Resistance of Top-Surface-Emitting Vertical-Cavity Diode Lasers

Using an approximate analytical approach described in the last quarterly report, we have tested sensitivity of thermal behavior to details of the device structure by considering a number of different heat source distributions. Our results demonstrate that the actual location of heat sources is of minor importance for the active-region temperature increase. The largest variation in temperature associated with redistribution of heat sources is less than 2.5%. Thus, thermal behavior of GaAs/AlGaAs proton-implanted top-surface-emitting lasers (PITSELS) can be approximated by lumping all sources of heat generated in the device into a single source located at the active region. The approximate analysis becomes therefore particularly simple, and thermal resistance R_{TH} of these devices can be easily calculated. Relatively high values of R_{TH} , obtained for lasers of typical active-region diameters ($\sim 20 \mu\text{m}$), are a direct consequence of the p-side up configuration.

During the next quarter, we plan to expand the current approach to include long-wavelength VCSELs and investigate the implications of the poor thermal conductivity of the quaternary layers. (Osinski)

Thermal Properties of Proton-Implanted Top-Surface-Emitting Lasers (PITSELS)

Thermal properties of VCSELs are very sensitive to details of the device design. We have therefore used the finite-element method to investigate temperature profiles, isotherms, and heat flow mechanisms in proton-implanted top-surface-emitting lasers (PITSELS). The results indicate that even close to threshold, radial heat flow plays a very important role in thermal dissipation. By the same token, while improving thermal characteristics of individual emitters, the radial heat flow will result in unacceptably high thermal crosstalk in densely-packed two-dimensional arrays of PITSELS. (Osinski)

Electrical Properties of PITSELS

Earlier analysis of spreading resistance in proton-implanted top-surface-emitting lasers (PITSELS), described in the last quarterly report, has been improved by allowing for anisotropic electrical resistivity in the spreading layer. As previously, three different top-contact geometries have been considered: annular, circular, and broad-area. Closed-form analytical solutions have been obtained for each case. The results support earlier conclusions

that low values of series resistance can be achieved by combining the broad-area or circular contact configuration with sufficiently large active-region diameters. (Osinski)

Wavelength Graded Resonant-Periodic-Gain Lasers

Dense wavelength division multiplexing (WDM) is a potential solution for the increased utilization of the terahertz bandwidth of optical fibers. One possible implementation of a WDM light source is a two-dimensional VCSEL array with uniformly graded emission wavelengths. We have achieved spatially graded lasing spectra using MOCVD-grown resonant-periodic-gain VCSELs. Samples were grown in a low-pressure horizontal-flow reactor. (Osinski, Malloy, and Hersee)

STANFORD UNIVERSITY

Visible Light Sources:

Phase modulation

In an effort to more fully understand the nature of phase modulation due to excitonic effects, we performed simulations of the behavior of exciton resonances in modulator structures. By performing the Kramers-Kronig transformation on measured exciton absorption spectra, we were able to obtain data displaying the effective refractive index of a quantum well versus wavelength for varying biases. We then utilized a matrix technique to solve Maxwell's equations for a multi-layer vertical cavity Fabry-Perot structure containing quantum wells described by the measured absorption data and the subsequently calculated refractive indices.

By operating between two points on opposite sides of the zero-reflectivity condition, we can obtain a modulation that does not have a reflectivity change between *on* and *off* states, but will change phase by 180 degrees plus a parasitic amount determined by the refractive index shift of the quantum well. However, at certain wavelengths, the relative phase of the exciton under applied bias and without bias can be zero--as seen by the symmetry in the exciton and in the Kramers-Kronig relations. Thus we can obtain a phase-flip switch with exactly 180 degrees phase change.

The device simulated has an 8-pair $\text{Al}_{0.33}\text{Ga}_{0.67}\text{As}/\text{AlAs}$ mirror, and a similarly configured 28.5 pair bottom mirror surrounding 92 75-Å GaAs quantum wells with 35-Å barriers. The Fabry-Perot dip is shifted to longer wavelength at 30 V. This is caused by the refractive index change associated with the exciton at this bias. However, as higher bias is applied, the Fabry-Perot dip is shifted to the same wavelength as at zero bias. This implies an equal effective cavity length and a zero relative phase change. The device shows about 50% reflectivity at low and high bias and a 180 degree phase change. An array of such devices could be used to make a controllable diffraction grating, which could be used for

such applications as beam steering. Furthermore, two dimensional arrays could be used for performing Fourier transforms, laser focusing, or complex optical interconnect schemes. (Harris)

Resonant Surface Emitting SHG

We continue to try to demonstrate surface emitting SHG in a vertical cavity. Although the waveguides fabricated earlier weren't entirely satisfactory, due to their high loss, we still believed that if enough light could be coupled into the sample, we'd be able to see red light. To that end, a dedicated endfiring station for this work was built, using new components for the most part. The new components were necessary because few of the necessary items could be borrowed, and those that could were either in bad condition or subject to reclamation. Another consideration is that the laser we are using is relatively low power (80 mW CW), so losing 5% of the power here and there due to inappropriate mirrors, damaged microscope objectives, etc. is not acceptable. However, there was still no red light, so we plan to use a more powerful laser. (Harris, Fejer)

MOCVD Growth and Processing

We have continued to investigate MOCVD growth and processing techniques required for the fabrication of laterally patterned II-VI layers for second harmonic generation. In particular, we have improved the quality of regrown <111> CdTe on GaAs after photolithography and etching of II-VI layers. Earlier this year we developed a new *in-situ* cleaning technique suitable for regrowth of <100>-oriented CdTe. For the device structure of interest however, it is desirable to grow the <100> material first, which requires regrowth of <111> CdTe. Since that time, we have found that regrowth of <111>-oriented CdTe is more sensitive to surface preparation. These problems have been addressed by modification of the wet chemical cleaning procedure prior to <111> CdTe regrowth. Photolithographic patterning of 10, 5, and 2.5 μm stripes of <100> CdTe on GaAs has been achieved using a KI:I:HBr etch. (Gibbons, Hoyt)

CALIFORNIA INSTITUTE OF TECHNOLOGY

The OMVPE reactor for our quantum-structure work with DEGaCl selective epitaxy, located at the NASA Jet Propulsion Laboratory, has been modified extensively to meet the rigorous requirements of quaternary compound InGaAsP growth and to improve the current AlGaAs growth characteristics.

A new main gas-injection manifold has been installed to incorporate more precursor sources and to improve gas handling characteristics. It accommodates up to twelve different sources with better pressure equalization. Extensive leak testing has been performed on the system to ensure the highest safety margin after these modifications. Initial growths of test layers are successful.

We also investigated the highly nondegenerate four-wave mixing in a 1.5- μm , compressively strained, multi-quantum-well traveling-wave optical amplifier at detuning frequencies up to 600 GHz. In this experiment, three tunable Erbium-doped fiber ring lasers were employed as pump, probe, and local oscillators, and the four-wave mixing signal was heterodyne detected by mixing the signal with the fiber-laser local oscillator. A gain nonlinearity with a characteristic relaxation time of 650 fs was determined from the experimental data, and the nonlinear gain coefficient was estimated to be $4.3 \times 10^{-23} \text{m}^3$. Dynamic carrier heating is concluded to be the major source of nonlinear gain in this device at the wavelengths investigated. (Vahala)

Accession For	
NTIS GRA&I	<input checked="" type="checkbox"/>
DTIC TAB	<input type="checkbox"/>
Unannounced	<input type="checkbox"/>
Justification	
By	
Distribution/	
Availability Codes	
Dist	Avail and/or Special
A-1	

**END
FILMED**

DATE:

4-93

DTIC